

# miRNA-26b suppresses the TGF- $\beta$ 2-induced progression of HLE-B3 cells *via* the PI3K/Akt pathway

En Shi<sup>1</sup>, Xiang-Nan Ye<sup>2</sup>, Liu-Yi Xie<sup>3</sup>

<sup>1</sup>Department of Ophthalmology, Ningbo Eye Hospital, Ningbo 315040, Zhejiang Province, China

<sup>2</sup>Department of Ophthalmology, Ningbo Medical Center Lihuli Hospital, Ningbo 315041, Zhejiang Province, China

<sup>3</sup>Department of Ophthalmology, Beilun District People's Hospital, Ningbo 315826, Zhejiang Province, China

**Correspondence to:** En Shi. 599 Beimingcheng Road, Yinzhou District, Ningbo 315040, Zhejiang Province, China. shienmr@163.com

Received: 2020-09-23 Accepted: 2021-04-23

## Abstract

• **AIM:** To study the effect of miR-26b on lens epithelial cells induced by transforming growth factor beta (TGF- $\beta$ ) 2 and the underlying signaling pathways.

• **METHODS:** Human lens epithelial cell line B-3 (HLE-B3) was incubated with TGF- $\beta$ 2 (5 ng/mL) and then transfected with miR-26b mimics. The expression of miR-26b was determined using quantitative reverse transcriptase polymerase chain reaction (qRT-PCR), while 5'-bromodeoxyuridine (BrdU) and wound-healing assays were used to measure the growth and migration of HLE-B3 cells, respectively. The expression of epithelial-mesenchymal transition (EMT) markers and the activity of the phosphatidylinositol 3-kinase (PI3K)/Akt pathway were measured by Western blotting assay and immunofluorescence staining. Electron microscopy was also used to observe cellular morphology.

• **RESULTS:** The expression levels of miR-26b were significantly reduced in human posterior capsular opacification-attached lens tissue and TGF- $\beta$ 2-stimulated HLE-B3 cells. In the presence of TGF- $\beta$ 2, the growth, migration, and EMT of HLE-B3 cells were distinctly enhanced; these effects were attenuated by the administration of miR-26b mimics. Furthermore, the overexpression of miR-26b significantly reduced upregulation of the PI3K/Akt pathway when stimulated by TGF- $\beta$ 2 in HLE-B3 cells. Moreover, the addition of an activator (740 Y-P) led to the upregulation of the PI3K/Akt pathway and abolished the protective effect of miR-26b on the HLE-B3 cells that was mediated by TGF- $\beta$ 2.

• **CONCLUSION:** The miR-26b suppresses TGF- $\beta$ 2-induced growth, migration, and EMT in HLE-B3 cells by regulating the PI3K/Akt signaling pathway.

• **KEYWORDS:** posterior capsule opacification; miRNA-26b; proliferation; migration; epithelial-mesenchymal transition

**DOI:10.18240/ijo.2021.09.09**

**Citation:** Shi E, Ye XN, Xie LY. miRNA-26b suppresses the TGF- $\beta$ 2-induced progression of HLE-B3 cells *via* the PI3K/Akt pathway. *Int J Ophthalmol* 2021;14(9):1350-1358

## INTRODUCTION

With an aging global population, the incidence of cataract, the predominant reason for blindness, has been gradually rising<sup>[1]</sup>. Surgery is the main treatment of cataract; the purpose is to remove the turbid lens and implant intraocular lens. However, this procedure is often accompanied by a subsequent reduction in vision<sup>[2]</sup>. The major complication associated with this surgery is posterior capsule opacification (PCO) caused by the proliferation, migration, and fibrogenesis of the remaining lens epithelial cells (LECs); this process can bring a heavy burden upon patients<sup>[3-4]</sup>. The incidence of PCO is approximately 50% in adults 2-5y after cataract surgery while the rate of Nd:YAG laser capsulotomy is approximately 24% 5y after cataract surgery<sup>[5-6]</sup>; collectively, these processes can cause a significant loss of vision. While previous research has enhanced our understanding of the pathophysiological processes involved with PCO<sup>[7-8]</sup>, the underlying molecular and cellular mechanisms and pathways associated with the development of PCO has yet to be elucidated<sup>[9]</sup>.

MicroRNAs (miRNAs) are defined as a type of non-coding single-stranded miRNA composed of 21-25 nucleotides<sup>[10]</sup> that can specifically bind to the non-coding 3'-UTR of target genes at the post-transcriptional and translational levels and subsequently modulate the expression of target genes by blocking translation or by inducing their degradation<sup>[10-11]</sup>. Numerous studies have reported that miRNA can be aberrantly expressed in the cornea, aqueous humor, lens and retina, and that this process is related to the occurrence of numerous diseases of the lens, including congenital cataract, age-induced cataract, diabetes-induced cataract and PCO<sup>[12-15]</sup>. Furthermore,

miR-26b has been demonstrated to interfere with the proliferation, migration, and epithelial-mesenchymal transition (EMT) of LECs induced by transforming growth factor beta (TGF- $\beta$ ) 2<sup>[16]</sup>; these processes can then lead to PCO. However, the precise mechanism underlying the effects of miR-26b on the development of PCO, particularly with regards to signaling pathways have yet to be elucidated.

It is now well established that TGF- $\beta$  can promote or suppress the proliferation and migration of various cells and can trigger aberrant changes in the morphology of lenses that imitate the characteristics of PCO and that TGF- $\beta$ 2 is the most potent form of TGF- $\beta$ <sup>[17-18]</sup>. The EMT model of LEC has been extensively studied as a cell model of cataract formation, including the mixture of anterior and posterior capsule<sup>[19-20]</sup>. Recent studies suggest that TGF- $\beta$ 2-driven proliferation or migration is associated with the activation of phosphatidylinositol 3-kinase (PI3K) and protein kinase B (PKB), also known as the PI3K/Akt pathway<sup>[19,21]</sup>. Moreover, the PI3K/Akt pathway plays a critical role in regulating different life-cycle events in LEC, including cell proliferation, migration, and EMT<sup>[19,22-23]</sup>. Therefore, the PI3K/Akt pathway could represent a promising therapeutic target for PCO.

In this study, we investigated the actions of miR-26b on growth, migration, and EMT in human lens epithelial cell line B-3 (HLE-B3) cells activated by TGF- $\beta$ 2. We also investigated the phosphorylation of PI3K and Akt to investigate whether the PI3K/Akt pathway is implicated in this process. In addition, we used 740 Y-P, an activator of the PI3K/Akt pathway, to investigate the precise mechanisms associated with the action of miR-26b on the development of PCO in order to provide a more accurate target for the clinical therapy of PCO.

## MATERIALS AND METHODS

**Ethical Approval** This study was approved by the Ethics Committee of the Hospital in Ningbo Provincial and all experimental processes were conducted in accordance with the Declaration of Helsinki. All participants provide informed written consent.

**Clinical Specimens and Cell Culture** Fresh human PCO-attached samples were collected from eight patients receiving surgical of turbid posterior capsular tissue removing at the Ningbo Eye Hospital (Ningbo, China). All patients were diagnosed as PCO, which were then graded: grade I in 2 cases, grade II in 4 cases, grade III in 2 cases, no other eye diseases. Age of the patients were ranged from 53 to 78 years old. The posterior capsule tissues of PCO patients were collected, cleaned with sterile normal saline, and then stored in a refrigerator at -20°C until to use. Similarly, four normal specimens of posterior capsular tissue were obtained from healthy subjects *via* the Eye Bank of Ningbo Eye Hospital (Ningbo, China).

The HLE-B3 was obtained from the Cell Bank Type Culture Collection of the Chinese Academy of Sciences (Shanghai, China). Dulbecco's modified Eagles media (DMEM) (Mediatech, Herndon, VA, USA), containing 10% fetal bovine serum (FBS; GIBCO Invitrogen, USA), was used to culture the cells, which were then placed in a 5% CO<sub>2</sub>-humidified incubator at 37°C. Cells were passaged with a 3:1 ratio when they reached 70%-80% confluency and cells from the third generation were used for experimental studies.

**Cell Transfection and Groupings** HLE-B3 cells were placed in 24-well plates (Costar, High Wycombe, UK) at a density of 1×10<sup>4</sup> cells/well and cultured at 37°C with 5% CO<sub>2</sub> for 24h. Subsequently, we mixed 0.4 nmol of miR-26b mimics (5'-ACAAUGUUCAUCGGUGUGGA-3') or control plasmid (mimic-NC; 5'-AUGCAUCCGGUAGGCAUGAUG-3') with 15  $\mu$ L Lipofectamine 2000 (Invitrogen, USA) and transfected these into HLE-B3 cells in accordance with the manufacturer's protocols. After 24h, the supernatant was discarded and replaced with fresh medium. The miR-26b mimics plasmid, as well as the negative mimic-NC, were provided by GenePharma (Shanghai, China).

Seven groups were included in our study, as follows: 1) Control group: HLE-B3 cells cultured routinely without any treatment; 2) TGF- $\beta$ 2 group: HLE-B3 cells treated with TGF- $\beta$ 2 (5 ng/mL, Cell Signaling, Danvers, MA, USA); 3) TGF- $\beta$ 2+miR-26b mimic group: HLE-B3 cells treated with miR-26b mimics and cultured with 5 ng/mL TGF- $\beta$ 2; 4) TGF- $\beta$ 2+mimic-NC group: HLE-B3 cells cultured with miR-26b negative control plasmid and administered with 5 ng/mL TGF- $\beta$ 2; 5) mimic-NC+saline group: HLE-B3 cells incubated with miR-26b negative control plasmid and cultured with 5 ng/mL TGF- $\beta$ 2 and 50  $\mu$ g/mL saline; 6) miR-26b mimic+saline group: HLE-B3 cells transfected with miR-26b mimics, and then incubated with 5 ng/mL TGF- $\beta$ 2 and 50  $\mu$ g/mL saline; 7) miR-26b mimic+740 Y-P group: HLE-B3 cells transfected with miR-26b mimics, followed by culture with 5 ng/mL TGF- $\beta$ 2 and 740 Y-P (50  $\mu$ g/mL, TocrisBioscience, Ellisville, MO, USA), an activator of the PI3K/Akt pathway (50  $\mu$ g/mL, TocrisBioscience, Ellisville, MO, USA).

**Quantitative Reverse Transcriptase Polymerase Chain Reaction** TRIzol reagent (Gibco BRL, Gaithersburg, MD, USA) was used to extract total RNA from tissues or HLE-B3 cells. RNA integrity was assessed by spectrophotometry (ND-1000, NanoDrop, Thermo Fisher Scientific Inc., MA, USA). A Taqman MicroRNA Reverse Transcription Kit (Thermo Fisher Scientific, MA, USA) was then used to obtain cDNA in accordance with the manufacturer's protocols. A SYBR Premix Ex TaqTM (TaKaRa, Otsu, Shiga, Japan) was used to perform quantitative reverse transcriptase polymerase chain reaction (qRT-PCR), and the relative

expression of miR-26b was normalized to the levels of U6 small nuclear RNA (snRNA). The sense primer for miR-26b was 5'-GGGACCCAGTTCAAGTAATTCAGG-3' and the antisense primer for miR-26b was 5'-TTTGCACTAGCACATT-3'. The sense primer for U6 was 5'-CTCGCTTCGGCAGCACA-3' and the antisense primer for U6 was 5'-AACG-CTTCACGAATTTGCGT-3'. The  $2^{-\Delta\Delta Ct}$  method was used to calculate relative gene expression.

**BrdU Incorporation Assay** Cells transfected with miR-26b mimics or mimic-NC were seeded into 96-well plates at a density of  $5 \times 10^4$  cells/well and cultured in DMEM containing 10% FBS. Instead of the primary culture medium, fresh medium was used to culture the cells overnight; this was followed by stimulation with and without 740 Y-P (50  $\mu\text{g}/\text{mL}$ ) for 30 min followed by TGF- $\beta$ 2 (5 ng/mL) treatment for 24 and 48h. Then, cells were labeled with 10  $\mu\text{mol}/\text{L}$  5-bromo-2'-deoxyuridine (BrdU; Sigma-Aldrich, St. Louis, MO, USA) for 2h. After fixation in 0.4% paraformaldehyde for 20min, and a washing step in PBS, the cells were then treated with 1.5 mol/L HCl for 10min. Subsequently, cells were cultured with mouse monoclonal anti-BrdU antibody with fluorescein isothiocyanate (Roche, Indianapolis, IN, USA) for 2h and then cultured with a goat anti-mouse secondary antibody labeled by fluorescein isothiocyanate (FITC; ab6785, 1:1000, Abcam, UK) for 1h. Cells were washed with PBS 3 times before each experimental procedure. In order to identify cell nuclei, we added 1  $\mu\text{g}/\text{mL}$  of 4', 6-diamino-2-phenylindole (DAPI; Santa Cruz, California, USA) as a counterstain. Fluorescence was then detected by fluorescent light microscopy (Olympus, BX 51, Japan).

**Wound-Healing Assay** HLE-B3 cells from each group (transfected with miR-26b mimics or mimic-NC) were placed in 24-well plates at a density of  $5 \times 10^4$  cells per well. After 24h of routine culture, the cells reached approximately 90% confluency in each well. We then added serum-free medium containing 0.2% bovine serum albumin (BSA) instead of the normal medium and incubated the cells overnight. The next morning, 740 Y-P (50  $\mu\text{g}/\text{mL}$ ) or saline were added and incubated with the cells for 30min. Then, a sterile pipette tip (20  $\mu\text{L}$ ) was used to scrape the confluent monolayers of the HLE-B3 cells to create a gap that was approximately 1.0 mm. Detached cells and debris were then removed by carefully washing the wounded monolayers with PBS. Then, the cells were grown in fresh medium with or without TGF- $\beta$ 2 (5 ng/mL). The wounds in each well were photographed at 0 and 48h using an inverted microscope (40 $\times$ ; X81; Olympus, Tokyo, Japan). Image J software (National Institutes of Health, Bethesda, MD, USA) was then used to determine the length of the remaining gap in each image. These experiments were carried out in triplicate.

**Western Blot Analysis** HLE-B3 cells were harvested from each group and lysed in RIPA buffer for 30min on ice. The lysed solutions were then centrifuged at 12 000 $\times$ g for 10min at 4°C to yield a supernatant that contained total cellular proteins. Protein concentrations were then determined using the bicinchoninic acid protein assay kit (Pierce, Rockford, IL., USA). Subsequently, protein samples (40  $\mu\text{g}$ ) were separated by 10% SDS-polyacrylamide gel (SDS-PAGE) and electrotransferred to polyvinylidene difluoride membranes (Millipore, Milford, Mass., USA). Subsequently, 5% skimmed milk in TBS buffer (containing 0.05% Tween-20) was used to block the membranes at room temperature for 2h. The membranes were then incubated overnight with a range of primary antibodies at 4°C: anti-E-cadherin (ab15148, 1:500), anti-cytokeratin (ab53280, 1:10 000), anti-fibronectin (ab268021, 1:1000), anti-vimentin (ab92547, 1:1000), anti-TGF- $\beta$ 2 (ab113670, 1:2000), anti-p-Smad2 (ab53100, 1:300), anti-Smad2 (ab33875, 1:1000), anti-p-Smad3 (ab52903, 1:2000), anti-Smad3 (ab40854, 1:1000), anti-p-Akt (ab81283, 1:5000), anti-Akt (ab8805, 1:500), anti-p-PI3K (ab182651, 1:500), anti-PI3K (ab32089, 1:1000) and anti-glyceraldehyde-3-phosphate dehydrogenase (GAPDH; ab8245, 1:500). All antibodies were purchased from Abcam Corporation (Abcam, UK). Afterwards, the membranes were washed three times with PBS and cultured with goat anti-mouse secondary antibody IgG (labeled with horseradish peroxidase; 1:1000; Santa Cruz, USA) at room temperature for 2h. Finally, the membranes were visualized by enhanced electrogenerated chemiluminescence (ECL, Santa Cruz Biotechnology). Images were captured by Image J software and relative protein expression was normalized to that of GAPDH.

**Immunofluorescence** HLE-B3 cells (transfected with miR-26b mimics or mimic-NC) were seeded in culture plates ( $5 \times 10^4$  cells/well) containing four chambers of polystyrene wells (BD Bioscience, Bedford, MA, USA) and incubated for 48h. Then, the normal medium was removed and replaced with serum-free medium, and the cells cultured overnight. Cells were then cultured with or without 740 Y-P (50  $\mu\text{g}/\text{mL}$ ) for 30min followed by a 24h period of culture with or without TGF- $\beta$ 2 (5 ng/mL). Subsequently, the cells were once in PBS and fixed with 1% polyfluoroalkoxy (PFA) at room temperature for 20min. Next, 0.1% Triton X-100 was used to permeabilize the cells for 15min. Cells were then washed in PBS, and 1% BSA/PBS was used to block the cells for 30min. Then, the cells were cultured overnight at 4°C with a range of primary antibodies: rabbit E-cadherin antibody (ab40772, 1:500), rabbit cytokeratin antibody (ab53280, 1:100), rabbit fibronectin antibody (ab23750, 1:40), and rabbit vimentin antibody (ab92547, 1:250). All antibodies were obtained from Abcam Corporation (Abcam, UK) and diluted in 1% BSA/PBS.

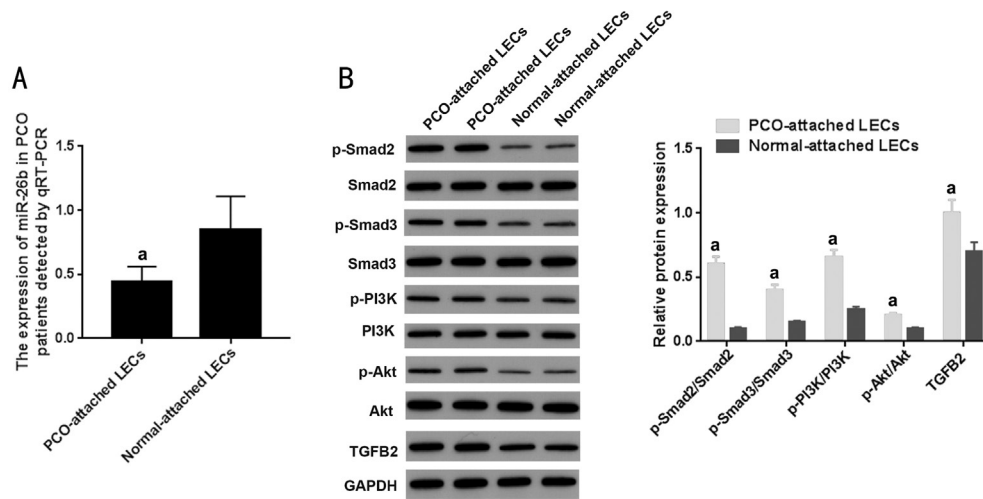


**Figure 1** The miR-26b expression and the relative activities of the TGF-β2/Smad and PI3K/Akt pathway in PCO patients A: The expression of miR-26b in PCO patients detected by qRT-PCR; B: The levels of TGF-β2, p-Smad2, Smad2, p-Smad3, Smad3, p-PI3K, PI3K, p-Akt, and Akt proteins in PCO patients determined by Western blot assay. Compared to the normal-attached LECs group, <sup>a</sup>*P*<0.05.

Next, the cells were washed in PBS and treated with FITC-conjugated goat anti-rabbit IgG secondary antibody (ab6717, 1:1000, Abcam, UK) diluted in 1% BSA/PBS for 1h at 37°C. Finally, the cells were placed on slides and counterstained with DAPI (Santa Cruz, California, USA). Digital images were then captured using an Olympus FV1000 confocal microscope (Tokyo, Japan).

**Scanning Electron Microscopy** After 24h of treatment, HLE-B3 cells were harvested from each group during the phase of logarithmic growth. These were washed three times in PBS. Then, cells were placed onto slides and fixed with 2.5% glutaraldehyde for 1h. The cells were washed again in PBS and then dehydrated in a gradient series of ethanol concentrations. Finally, the cells were permeabilized by isoamyl acetate for 3h. Finally, morphological changes were observed by scanning electron microscopy.

**Statistical Analysis** Data are represented as mean±standard deviation (SD) and were analyzed with SPSS version 19.0 software (SPSS, Chicago, Illinois, USA). Data that were not normally distributed were analyzed by the nonparametric Mann-Whitney *U* Test. The Student's *t*-test, and the Chi-squared test were used to analyze differences between the two groups. One-way analysis of variance (ANOVA), followed by a post-hoc test, was used to analyze the differences between multiple groups. *P*<0.05 was considered as statistically significant.

## RESULTS

**Reduced Expression of miR-26b and Activation of the TGF-β2/Smad and PI3K/Akt Pathway in PCO Patients** We collected eight lens tissues from patients with PCO and four normal lens tissues from healthy subjects in order to investigate the expression of miR-26b and the activities of the TGF-β2/Smad and PI3K/Akt pathways in PCO. The qRT-PCR showed that the expression of miR-26b in PCO-attached lens tissue

was significantly reduced when compared to normal tissues (*P*<0.05, Figure 1A). Furthermore, the protein levels ratio of TGF-β2, p-Smad2/Smad2, p-Smad3/Smad3, p-PI3K/PI3K, and p-Akt/Akt, in PCO-attached LECs were significantly elevated (*P*<0.05, Figure 1B), as demonstrated by western blot analysis. This data illustrated that the expression of miR-26b was reduced in patients with PCO, while the activities of the TGF-β2/Smad and PI3K/Akt pathways were upregulated.

**MiR-26b Inhibited the Proliferation, Migration, and EMT of HLE-B3 cells Stimulated by TGF-β2** To explore whether miR-26b was involved in the development of PCO, we cultured HLE-B3 *in vitro* and used TGF-β2 to induce fibrotic changes in these cells. We also overexpressed miR-26b to evaluate its effects on fibrotic changes in HLE-B3 cells. As detected by qRT-PCR, the expression levels of miR-26b in the TGF-β2 group were significantly reduced when compared to the control group. In contrast, the expression levels of miR-26b in the TGF-β2+miR-26b mimic group was significantly higher compared to the TGF-β2+mimic-NC group (all *P*<0.05, Figure 2A). Furthermore, we used the BrdU assay to evaluate the proliferative ability of HLE-B3 cells in each group; these assays indicated that there were no significant differences in the proliferation between the four groups at 0h (*P*>0.05). However, at 48h, the proliferative ability of HLE-B3 cells in the TGF-β2 group was significantly weaker than the control group (*P*<0.05). Notably, the administration of miR-26b mimics in the TGF-β2 + miR-26b mimic group led to a significant suppression in the reduced proliferative ability of HLE-B3 cells mediated by TGF-β2 when compared with the TGF-β2 + mimic-NC group (*P*<0.05, Figure 2B).

**MiR-26b Inhibited the Migration and EMT of HLE-B3 Cells Stimulated by TGF-β2** Moreover, the migration and EMT ability were then be investigated. Scratch-wound

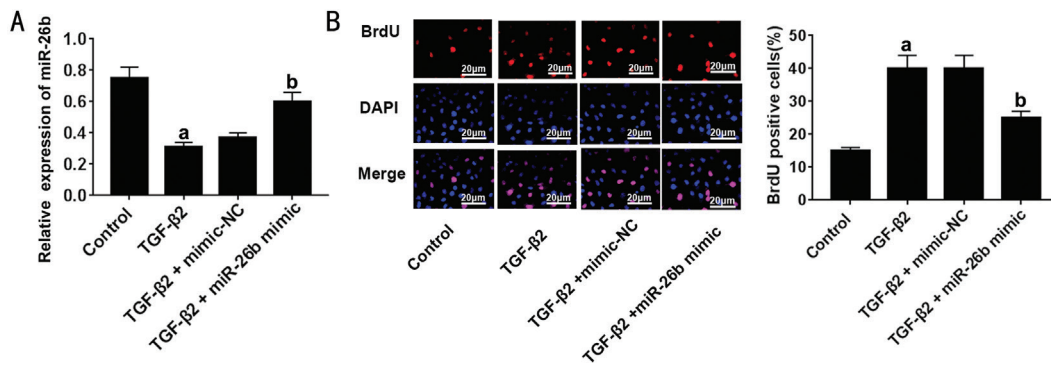


**Figure 2** The effects of miR-26b on the proliferation, migration, and epithelial-mesenchymal transformation of HLE-B3 cells induced by TGF-β2. A: The expression of miR-26b in HLE-B3 cells determined by qRT-PCR; B: The proliferative ability of HLE-B3 cells detected by BrdU incorporation assays. Compared to the control group, <sup>a</sup> $P < 0.05$ ; Compared to the TGF-β2 + mimic-NC group, <sup>b</sup> $P < 0.05$ .

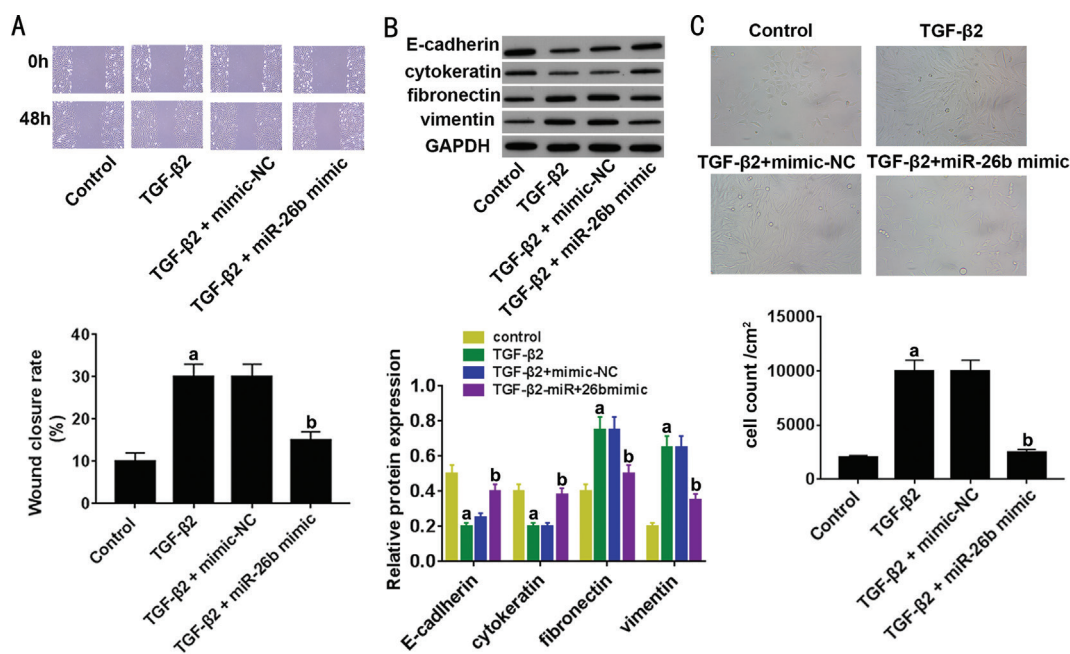


**Figure 3** The effects of miR-26b on the migration and epithelial-mesenchymal transformation of HLE-B3 cells induced by TGF-β2. A: The migration ability of HLE-B3 cells determined by scratch-wound healing assays; B: The protein levels of E-cadherin, cytokeratin, fibronectin, and vimentin in HLE-B3 cells detected by Western blot analysis; C: The morphology of HLE-B3 cells, as observed by inverted microscopy. Compared to the control group, <sup>a</sup> $P < 0.05$ ; Compared to the TGF-β2 + mimic-NC group, <sup>b</sup> $P < 0.05$ .

healing assays were used to evaluate the migration ability of HLE-B3 cells in each group. As seen with proliferative ability, the ability of HLE-B3 cells migration at 48h in the TGF-β2 group had declined significantly; the administration of miR-26b mimics reversed this effect (all  $P < 0.05$ , Figure 3A). EMT was investigated in HLE-B3 cells by Western blotting and immunofluorescence using a range of EMT markers, including the absence of an epithelial phenotype (reductions in E-cadherin and cytokeratin), the generation of an interstitial phenotype (increased levels of fibronectin), and the production of fibrosis markers (increased levels of vimentin). As illustrated in Figure 3B, compared with the control group, the expression levels of E-cadherin and cytokeratin were significantly reduced while the expression levels of fibronectin and vimentin were

significantly increased in the TGF-β2 group (all  $P < 0.05$ ). Compared with the TGF-β2+mimic-NC group, the levels of E-cadherin and cytokeratin were significantly elevated in the TGF-β2+miR-26b mimic group while the levels of fibronectin and vimentin were significantly reduced (all  $P < 0.05$ ). Cell morphology was observed by inverted microscopy. Compared with the control group, the cells in the TGF-β2 group changed from a single-layer polygonal shape to a long spindle shape and showed fibrosis-like changes. The administration of miR-26b mimics clearly inhibited the fibrosis-like changes of HLE-B3 cells stimulated by TGF-β2 (Figure 3C). These results indicated that TGF-β2 can promote the growth, migration, and EMT of HLE-B3 cells, whereas the overexpression of miR-26b reverses the enhancing effect of

TGF- $\beta$ 2 on the proliferation, migration, and EMT, on HLE-B3 cells.

**MiR-26b Inhibited Activation of the PI3K/Akt Pathway Induced by TGF $\beta$ -2 in HLE-B3 Cells** Studies have confirmed that TGF- $\beta$ 2-mediated proliferation or migration is strongly related to the activity of the PI3K/Akt pathway<sup>[19,21]</sup>. We investigated how the activity of the PI3K/Akt pathway changes in HLE-B3 cells when stimulated by TGF- $\beta$ 2 and treated with miR-26b mimics. We found that the protein level ratios of p-PI3K/PI3K and p-Akt/Akt were significantly higher in the TGF- $\beta$ 2 group than in the control group (all  $P < 0.05$ ), while the ratios of p-PI3K/PI3K and p-Akt/Akt were lower in the TGF- $\beta$ 2+miR-26b mimic group than in the TGF- $\beta$ 2+mimic-NC group (all  $P < 0.05$ , Figure 4). This finding indicated that TGF- $\beta$ 2 treatment can induce significant activation of the PI3K/Akt pathway in HLE-B3 cells, while the activation effect of TGF- $\beta$ 2 upon the PI3K/Akt pathway was diminished by the transfected with of miR-26b mimics.

**MiR-26b Inhibited TGF- $\beta$ 2-induced Growth, Migration, and EMT in HLE-B3 Cells by Modulating the PI3K/Akt Pathway** To further explore whether miR-26b suppresses TGF- $\beta$ 2-triggered growth, migration, and EMT of HLE-B3 cells *via* the PI3K/Akt pathway, we incubated 740 Y-P with HLE-B3 cells transfected with miR-26b mimics to activate the PI3K/Akt pathway. As presented in Figure 5A, in contrast to the mimic-NC+saline group, the ratio of p-PI3K/PI3K, p-Akt/Akt were significantly reduced in the miR-26b mimic+saline group (all  $P < 0.05$ ). However, the ratios of p-PI3K/PI3K and p-Akt/Akt were significantly higher in the miR-26b mimic+740 Y-P group compared with the miR-26b mimic+saline group (all  $P < 0.05$ ). In addition, the abilities of the HLE-B3 cells of proliferate and migrate in the miR-26b mimic+saline group were notably weaker in the mimic-NC+saline group (all  $P < 0.05$ ). In contrast, the proliferation and migration ability of HLE-B3 cells in the miR-26b mimic+740 Y-P group were significantly enhanced when compared to the mimic-NC+saline group (all  $P < 0.05$ , Figure 5B). Therefore, our data indicated that miR-26b inhibited the TGF- $\beta$ 2-driven growth of HLE-B3 cells *via* inactivation of the PI3K/Akt pathway.

**MiR-26b Suppressed TGF- $\beta$ 2-induced EMT and Migration in HLE-B3 Cells by Modulating the PI3K/Akt Pathway** Then, the EMT and migration ability of HLE-B3 cells were studied, and the evident trends for the expression of EMT marker proteins were consistent with those for proliferative ability. This implied that the protein levels of E-cadherin and cytokeratin were significantly increased, and the levels of fibronectin and vimentin were significantly decreased in the miR-26b mimic+saline group. These tendencies were reversed

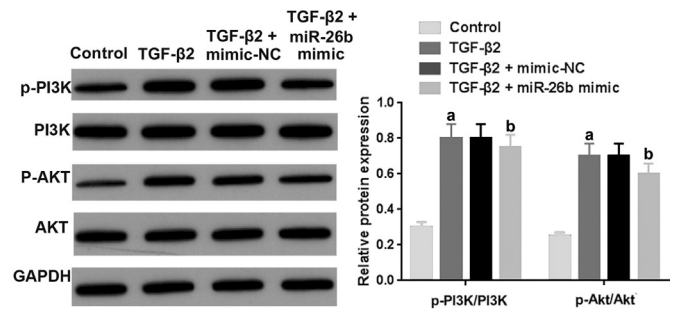


**Figure 4** The effect of miR-26b on the activity of the PI3K/Akt pathway in HLE-B3 cells induced by TGF- $\beta$ 2 The protein expression of p-PI3K, PI3K, p-Akt, and Akt in HLE-B3 cells measured by Western blot assay. Compared to the control group, <sup>a</sup> $P < 0.05$ ; Compared to the TGF- $\beta$ 2 + mimic-NC group, <sup>b</sup> $P < 0.05$ .

after the introduction of 740 Y-P in the miR-26b mimic+740 Y-P group ( $P < 0.05$ , Figure 6A). Next, the migration ability of HLE-B3 cells was measured. Compared with the mimic-NC+saline group, the migration ability of HLE-B3 cells was significantly decreased in the miR-26b mimic+saline group, while the ability was evidently rise up in the miR-26b mimic+740 Y-P group which treated with the activator of PI3K/Akt pathway by compared with the miR-26b mimic+saline group ( $P < 0.05$ , Figure 6B).

Moreover, the morphology of HLE-B3 cells supported the EMT results in that fibrosis-like changes of HLE-B3 cells in the miR-26b mimic+saline group were attenuated compared to the mimic-NC+saline group. However, the fibrosis-like changes of HLE-B3 cells in the miR-26b mimic+740 Y-P group were clearly aggravated compared to the mimic-NC+saline group (Figure 6C). Hence, we can believe that miR-26b inhibited the TGF- $\beta$ 2-driven EMT and migration of HLE-B3 cells *via* inactivity of the PI3K/Akt pathway.

## DISCUSSION

The EMT of LECs is an abnormal process of cell differentiation from epithelial-like cells to elongated fibroblast-like cells. This process can generate a significant amount of extracellular matrix, leading to the emergence of fibrotic plaques. This causes the posterior capsule to collapse and lose its transparency, ultimately leading to PCO and serious visual impairment<sup>[24-25]</sup>. According to statistics, the incidence of PCO in adults is 4.0%-13.6% within 1-3y of cataract surgery. In children, the incidence of PCO can reach 100%; this has been attributed to the strong proliferative ability of LECs in this age group<sup>[26-27]</sup>. PCO can cause serious harm to vision and is associated with a heavy economic burden. However, the precise molecular mechanisms underlying the development of PCO, especially with regards to signaling pathways, have yet to be fully elucidated. A better understanding of these mechanisms will help us to develop new strategies for the prevention of PCO.

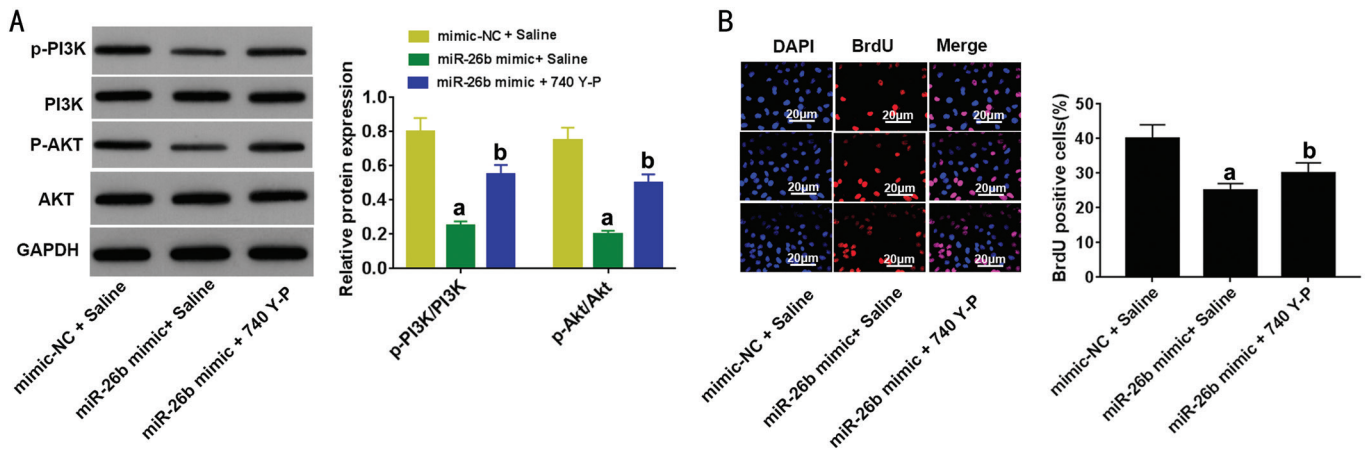


**Figure 5** MiR-26b inhibited TGF-β2-induced growth in HLE-B3 cells by regulating the PI3K/Akt pathway A: The protein expression of p-PI3K, PI3K, p-Akt, and Akt in HLE-B3 cells determined by Western blot assay; B: The proliferation ability of HLE-B3 cells detected by BrdU incorporation assays. Compared to the mimic-NC+saline group group, <sup>a</sup>*P*<0.05; Compared to the miR-26b mimic+ saline group, <sup>b</sup>*P*<0.05.

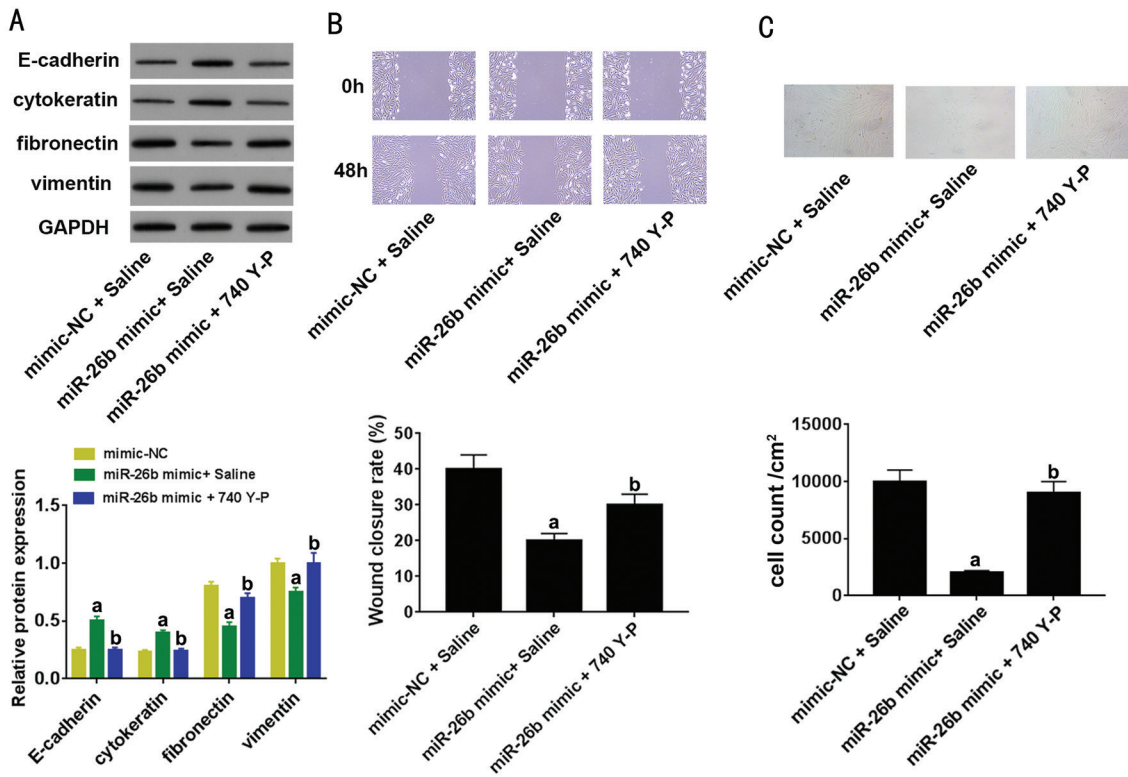


**Figure 6** MiR-26b inhibited TGF-β2-induced EMT and migration in HLE-B3 cells by regulating the PI3K/Akt pathway A: The protein expression of E-cadherin, cytokeratin, fibronectin and vimentin in HLE-B3 cells detected by Western blot analysis; B: The migration ability of HLE-B3 cells determined by scratch-wound healing assays; C: The morphology of HLE-B3 cells revealed by inverted microscopy. Compared to the mimic-NC+saline group group, <sup>a</sup>*P*<0.05; Compared to the miR-26b mimic+saline group, <sup>b</sup>*P*<0.05.

In order to create an *in vitro* model of PCO, we used TGF-β2 to trigger EMT in LECs. TGF-β2 is the most important regulatory factor for the lens in a variety of physiological and pathological states. TGF-β2 exists in an inactive latent form and exerts a critical role in the physiological differentiation of LECs<sup>[28-29]</sup>. Studies have indicated that the administration of TGF-β2 to HLE-B3 cells can result in morphological changes, weaker cell connections, and the increased expression of fibronectin, thus causing EMT<sup>[30-31]</sup>. Our research showed that TGF-β2 can

promote the proliferation and migration of HLE-B3 cells, and that TGF-β2 reduced the levels of E-cadherin, cytokeratin, and fibronectin proteins, while elevating the levels of vimentin protein. Furthermore, the morphology of HLE-B3 cells changed from a single-layer of cuboidal cells to spindle cells when examined by inverted microscopy. These findings were similar to those reported previously<sup>[16,30-31]</sup>. The regulatory role of miR-26b in lens fibrosis and PCO has received increasing levels of research attention over recent years.

For example, Dong *et al*<sup>[16]</sup> reported that miR-26b suppressed the growth, migration, and EMT of SRA01/04 cells, and that this was driven by TGF- $\beta$ 2 *via* the downregulation of Smad4 and COX-2. In another study, Chen *et al*<sup>[32]</sup> demonstrated that miR-26a and miR-26b inhibited the growth, migration, and EMT of LECs as well as lens fibrosis, *via* negative regulation of the Jagge-1/Notch signaling pathway. Another study suggested that epidermal growth factor (EGF) inhibits the upregulation of miR-26b induced by TGF- $\beta$ 2, then induces the expression of EZH2 and promotes EMT development of HLECs<sup>[33]</sup>. Indeed, our present data showed lower levels of miR-26b in PCO-attached lens tissue than normal-attached lens tissue. *In vitro*, miR-26b was significantly inhibited by TGF- $\beta$ 2, while obviously mitigating the proliferation, migration, and expression of EMT markers in HLE-B3 cells stimulated by TGF- $\beta$ 2. Furthermore, it was evident that the administration of miR-26b mimic prevented the morphology of HLE-B3 cells changing to spindle cells, thus indicating that miR-26b can be significantly modulated by TGF- $\beta$ 2 signaling and then confer an inhibitory effect on proliferation, migration, and EMT in HLE-B3 cells mediated by TGF- $\beta$ 2; these data are consistent with a previous study<sup>[16,32]</sup>. Furthermore, miR-26b mimics significantly attenuated activity of the PI3K/Akt pathway in HLE-B3 cells when stimulated by TGF- $\beta$ 2.

It is important that we understand the mechanisms downstream of miR-26b during EMT in HLE-B3 cells mediated by TGF- $\beta$ 2; the PI3K/Akt pathway has become the main focus of our attention. Previous studies have confirmed that activation of the PI3K/Akt pathway confers a critical effect on the TGF- $\beta$ 2-driven EMT process in HLE-B3 cells<sup>[19,34]</sup>. In addition, Du *et al*<sup>[35]</sup> reported that quercetin inhibits EMT in the SRA01/04 cell lines *via* the PI3K/Akt signal transduction pathway. Consequently, the TGF- $\beta$ 2/PI3K/Akt signaling pathways are implicated as key regulatory mechanisms in the pathological process of PCO and act by influencing the EMT of LECs. In this study, we found that the PI3K/Akt pathway was upregulated in PCO-attached lens tissue and TGF- $\beta$ 2-induced HLE-B3 cells. However, this activation in HLE-B3 cells was clearly inhibited by transfection with an miR-26b mimic. To further address whether miR-26b attenuates the enhanced growth, migration, and EMT of HLE-B3 cells stimulated by TGF- $\beta$ 2 through the PI3K/Akt pathway, we carried out experiments with 740 Y-P. We showed that the administration of 740 Y-P enhanced the ability of TGF- $\beta$ 2 to promote proliferation, migration, and EMT in HLE-B3 cells. Interestingly, 740 Y-P treatment significantly eliminated the suppressive effect of miR-26b on growth, migration, and EMT in HLE-B3 cells treated with TGF- $\beta$ 2. Therefore, we considered that miR-26b attenuated the stimulatory effect of TGF- $\beta$ 2 in growth, migration, and EMT in HLE-B3 cells

by deactivating the PI3K/Akt pathway. To the best of our knowledge, this is the first paper to report the molecular mechanisms underlying the action of miR-26b on TGF- $\beta$ 2-stimulated growth, migration, and EMT in HLE-B3 cells through the PI3K/Akt pathway. Consequently, it is evident that miR-26b may represent a promising target for the development of a novel therapeutic strategy for PCO.

In summary, we detected reduced expression levels of miR-26b in human PCO lens tissue and TGF- $\beta$ 2-induced HLE-B3 cells. The overexpression of miR-26b *in vitro* led to the inhibition of HLE-B3 cell proliferation, migration, and EMT; this occurred in parallel with the downregulation of the PI3K/Akt pathway. Notably, when the PI3K/Akt pathway was activated by 740 Y-P, there was a significant reduction in the inhibitory effect of miR-26b on growth, migration, and EMT in HLE-B3 cells. These results demonstrated that miR-26b may play a critical role in modulating the prognosis of HLE-B3 mediated by TGF- $\beta$ 2, probably through the PI3K/Akt pathway. Consequently, miR-26b represents a promising target for the development of a novel therapeutic strategy for PCO.

#### ACKNOWLEDGEMENTS

**Conflicts of Interest:** Shi E, None; Ye XN, None; Xie LY, None.

#### REFERENCES

- 1 Cataract - a leading cause of blindness. *JNMA J Nepal Med Assoc* 2007;46(167):I-II.
- 2 Sharma B, Abell RG, Arora T, Antony T, Vajpayee RB. Techniques of anterior capsulotomy in cataract surgery. *Indian J Ophthalmol* 2019;67(4):450-460.
- 3 Tang JM, Liu SH, Han YM, Wang R, Xia JY, Chen H, Lin QK. Surface modification of intraocular lenses via photodynamic coating for safe and effective PCO prevention. *J Mater Chem B* 2021;9(6):1546-1556.
- 4 Findl O, Buehl W, Bauer P, Sycha T. Interventions for preventing posterior capsule opacification. *Cochrane Database Syst Rev* 2010(2):CD003738.
- 5 Johansson B. Clinical consequences of acrylic intraocular lens material and design: Nd: YAG-laser capsulotomy rates in 3 x 300 eyes 5y after phacoemulsification. *Br J Ophthalmol* 2010;94(4):450-455.
- 6 Hiramatsu N, Nagai N, Kondo M, Imaizumi K, Sasaki H, Yamamoto N. Morphological comparison between three-dimensional structure of immortalized human lens epithelial cells and Soemmering's ring. *Med Mol Morphol* 2021;54(3):216-226.
- 7 Chen X, Yan H, Chen Y, Li G, Bin Y, Zhou X. Moderate oxidative stress promotes epithelial-mesenchymal transition in the lens epithelial cells via the TGF- $\beta$ /Smad and Wnt/ $\beta$ -catenin pathways. *Mol Cell Biochem* 2021;476(3):1631-1642.
- 8 Peng C, Wang YC, Ji LY, Kuang LJ, Yu ZY, Li HR, Zhang JS, Zhao JY. LncRNA-MALAT1/miRNA-204-5p/Smad4 axis regulates epithelial-mesenchymal transition, proliferation and migration of lens epithelial cells. *Curr Eye Res* 2021;46(8):1137-1147.

- 9 Guha R, Chowdhury S, Palui H, Mishra A, Basak S, Mandal TK, Hazra S, Konar A. Doxorubicin-loaded MePEG-PCL nanoparticles for prevention of posterior capsular opacification. *Nanomedicine* 2013;8(9):1415-1428.
- 10 He L, Hannon GJ. MicroRNAs: small RNAs with a big role in gene regulation. *Nat Rev Genet* 2004;5(7):522-531.
- 11 Bartel DP. MicroRNAs: genomics, biogenesis, mechanism, and function. *Cell* 2004;116(2):281-297.
- 12 Iliif BW, Riazuddin SA, Gottsch JD. A single-base substitution in the seed region of miR-184 causes EDICT syndrome. *Invest Ophthalmol Vis Sci* 2012;53(1):348-353.
- 13 Wu CR, Lin HT, Wang QL, Chen W, Luo HH, Chen WR, Zhang H. Discrepant expression of microRNAs in transparent and cataractous human lenses. *Invest Ophthalmol Vis Sci* 2012;53(7):3906-3912.
- 14 Feng D, Zhu N, Yu CY, Lou DH. MicroRNA-34a suppresses human lens epithelial cell proliferation and migration via downregulation of c-Met. *Clin Chim Acta* 2019;495:326-330.
- 15 Li H, Song H, Yuan XY, Li J, Tang H. miR-30a reverses TGF- $\beta$ 2-induced migration and EMT in posterior capsular opacification by targeting Smad2. *Mol Biol Rep* 2019;46(4):3899-3907.
- 16 Dong N, Xu B, Benya SR, Tang X. MiRNA-26b inhibits the proliferation, migration, and epithelial-mesenchymal transition of lens epithelial cells. *Mol Cell Biochem* 2014;396(1-2):229-238.
- 17 Yang YF, Ye YM, Lin XC, Wu KL, Yu MB. Inhibition of pirfenidone on TGF-beta2 induced proliferation, migration and epithelial-mesenchymal transition of human lens epithelial cells line SRA01/04. *PLoS One* 2013;8(2):e56837.
- 18 de Iongh RU, Wederell E, Lovicu FJ, McAvoy JW. Transforming growth factor-beta-induced epithelial-mesenchymal transition in the lens: a model for cataract formation. *Cells Tissues Organs* 2005;179(1-2):43-55.
- 19 Yao K, Ye PP, Tan J, Tang XJ, ShenTu XC. Involvement of PI3K/Akt pathway in TGF-beta2-mediated epithelial mesenchymal transition in human lens epithelial cells. *Ophthalmic Res* 2008;40(2):69-76.
- 20 Shirai K, Saika S, Tanaka T, Okada Y, Flanders KC, Ooshima A, Ohnishi Y. A new model of anterior subcapsular cataract: involvement of TGFbeta/Smad signaling. *Mol Vis* 2006;12:681-691.
- 21 Cao Q, Deji QZ, Liu YJ, Ye W, Zhaba WD, Jiang Q, Yan F. The role of mechanical stretch and TGF- $\beta$ 2 in epithelial-mesenchymal transition of retinal pigment epithelial cells. *Int J Ophthalmol* 2019;12(12):1832-1838.
- 22 Liegl R, Wertheimer C, Kernt M, Docheva D, Kampik A, Eibl-Lindner KH. Attenuation of human lens epithelial cell spreading, migration and contraction via downregulation of the PI3K/Akt pathway. *Graefes Arch Clin Exp Ophthalmol* 2014;252(2):285-292.
- 23 Jiang Q, Zhou CL, Bi ZG, Wan YS. EGF-induced cell migration is mediated by ERK and PI3K/AKT pathways in cultured human lens epithelial cells. *J Ocul Pharmacol Ther* 2006;22(2):93-102.
- 24 Raj SM, Vasavada AR, Johar SR, et al. Post-operative capsular opacification: a review. *Int J Biomed Sci* 2007;3(4):237-250.
- 25 Zheng DY, Song TT, Zhongliu XY, Wu MX, Liang JL, Liu YZ. Downregulation of transforming growth factor- $\beta$  type II receptor prohibit epithelial-to-mesenchymal transition in lens epithelium. *Mol Vis* 2012;18:1238-1246.
- 26 Schallhorn JM, Schallhorn SC, Teenan D, Hannan SJ, Pelouskova M, Venter JA. Incidence of intraoperative and early postoperative adverse events in a large cohort of consecutive refractive lens exchange procedures. *Am J Ophthalmol* 2019;208:406-414.
- 27 Shah GD, Vasavada AR, Praveen MR, Shah AR, Trivedi RH. Incidence and influence of posterior capsule striae on the development of posterior capsule opacification after 1-piece hydrophobic acrylic intraocular lens implantation. *J Cataract Refract Surg* 2012;38(2):202-207.
- 28 Li J, Tang X, Chen X. Comparative effects of TGF- $\beta$ 2/Smad2 and TGF- $\beta$ 2/Smad3 signaling pathways on proliferation, migration, and extracellular matrix production in a human lens cell line. *Exp Eye Res* 2011;92(3):173-179.
- 29 Boswell BA, VanSlyke JK, Musil LS. Regulation of lens gap junctions by Transforming Growth Factor beta. *Mol Biol Cell* 2010;21(10):1686-1697.
- 30 Lovicu FJ, Ang S, Chorazyczewska M, McAvoy JW. Deregulation of lens epithelial cell proliferation and differentiation during the development of TGFbeta-induced anterior subcapsular cataract. *Dev Neurosci* 2004;26(5-6):446-455.
- 31 Dwivedi DJ, Pino G, Banh A, Nathu Z, Howchin D, Margetts P, Sivak JG, West-Mays JA. Matrix metalloproteinase inhibitors suppress transforming growth factor- $\beta$ -induced subcapsular cataract formation. *Am J Pathol* 2006;168(1):69-79.
- 32 Chen XY, Xiao W, Chen WR, Liu XL, Wu MX, Bo Q, Luo Y, Ye SB, Cao YH, Liu YZ. MicroRNA-26a and -26b inhibit lens fibrosis and cataract by negatively regulating Jagged-1/Notch signaling pathway. *Cell Death Differ* 2017;24(11):1990.
- 33 Dong N, Xu B, Xu JM. EGF-mediated overexpression of myc attenuates miR-26b by recruiting HDAC3 to induce epithelial-mesenchymal transition of lens epithelial cells. *Biomed Res Int* 2018;2018:7148023.
- 34 Wilhelm J, Smistik Z, Mahelková G, Vytásek R. Redox regulation of proliferation of lens epithelial cells in culture. *Cell Biochem Funct* 2007;25(3):317-321.
- 35 Du L, Hao M, Li CC, Wu WY, Wang WW, Ma ZX, Yang TT, Zhang N, Isaac AT, Zhu X, Sun Y, Lu Q, Yin XX. Quercetin inhibited epithelial mesenchymal transition in diabetic rats, high-glucose-cultured lens, and SRA01/04 cells through transforming growth factor- $\beta$ 2/phosphoinositide 3-kinase/Akt pathway. *Mol Cell Endocrinol* 2017;452:44-56.